Spectroscopic (IR, UV–Vis, ^1H and ^{119}Sn NMR, Resonance Raman) Properties of $[(C_6H_5)_3EM(CO)_3(\alpha\text{-diimine})]$ (M = Mn, E = Ge, Sn, Pb; M = Re, E = Sn) Complexes and X-ray Structure of $[(C_6H_5)_3SnMn(CO)_3(t\text{-Bu-DAB})]$

RONALD R. ANDRÉA, WIM G. J. DE LANGE, DERK J. STUFKENS* and AD OSKAM

Anorganisch Chemisch Laboratorium, University of Amsterdam, J.H. van't Hoff Instituut, Nieuwe Achtergracht 166, 1018 WV Amsterdam, The Netherlands

(Received December 29, 1987)

Abstract

The X-ray structure of the title compound has been determined by the heavy-atom method and refined by means of block-diagonal least-squares calculations from 4598 independent reflections. The crystals are monoclinic, space group $P2_1/c$ with unit cell dimensions $a = 20.025(1)$, $b = 18.917(1)$, $c = 17.117(1)$ Å, $\beta = 112.120(0)°$ and $Z = 8$. The complex has a nearly octahedral geometry around the Mn atom. The Mn–Sn bond length is 2.70(1) Å and the two Mn–N bond lengths are 2.10(2) Å.

Infrared (IR), electronic absorption, ^1H and ^{119}Sn NMR and resonance Raman (rR) spectra are reported for the complexes $[(C_6H_5)_3EM(CO)_3(\alpha\text{-diimine})]$ (M = Mn, E = Ge, Sn, Pb; M = Re, E = Sn; α-diimine = 1,4-diaza-1,3-butadiene, pyridine-2-carbaldehyde-imine and 2,2′-bipyridine). The IR bands in the CO stretching region are assigned and the rR effect observed for one of these vibrations ($\nu(CO)_{ax}$) in the case of the Mn complexes is explained with a delocalization of the lowest MLCT state over this axial-carbonyl ligand.

Introduction

Low-valence transition metal complexes of α-diimine ligands are highly coloured due to the presence of low-energy metal to α-diimine charge transfer (MLCT) transitions [1–3]. For a series of d^6-$[M(CO)_4(\alpha\text{-diimine})]$ (M = Cr, Mo, W) [4, 5], d^7-$[(CO)_5MM'(CO)_3(\alpha\text{-diimine})]$ (M, M′ = Mn, Re) [6] and d^8-$[M(CO)_3(\alpha\text{-diimine})]$ (M = Fe, Ru) [7, 8] complexes, we have studied the spectroscopic and photochemical properties. In most cases the α-diimine ligands used are 1,4-diaza-1,3-butadiene (RN=CH–CH=NR; R–DAB)**, pyridine-2-carbaldehydeimine (C_5H_4N-2-CH=NR; R–PyCa), 2,2′-bipyridine (bipy) and 1,10-phenanthroline (phen). A close relationship was deduced for these complexes between their photochemical and photophysical behaviour and resonance Raman (rR) spectra, obtained by excitation into the low-energy MLCT band.

Of special interest are the results for the d^7 metal–metal bonded complexes $[(CO)_5MnMn(CO)_3(\alpha\text{-diimine})]$ which show two different photochemical reactions in 2-Me-THF depending on the temperature [9]. The main reaction at room temperature is a homolytic splitting of the metal–metal bond followed by combination of the radicals to form $[Mn_2(CO)_{10}]$ and $[Mn_2(CO)_6(\alpha\text{-diimine})_2]$. When the reaction is performed in the presence of a basic PR_3 ligand, a photocatalytic disproportionation of the parent compound into $[Mn(CO)_3(\alpha\text{-diimine})(PR_3)]^+$ and $[Mn(CO)_5]^-$ is observed with quantum yields higher than 10. When the photolysis reaction, however, takes place at 133 K, just above the glass-point of 2-Me-THF, photosubstitution of CO in the $Mn(CO)_3(\alpha\text{-diimine})$ fragment takes place followed by a disproportionation of the photoproduct into $[Mn(CO)_3(\alpha\text{-diimine})(S)]^+$ and $[Mn(CO)_5]^-$ upon raising the temperature [9a, b]. Now, in order to find out whether this remarkable behaviour is a general property of this type of metal–metal bonded complexes, we extended our studies to $[Fe_2(CO)_7(\alpha\text{-diimine})]$ [10], $[(CO)_4CoMn(CO)_3(\alpha\text{-diimine})]$ and $[(C_6H_5)_3EM(CO)_3(\alpha\text{-diimine})]$ (M = Mn, Re; E = Ge,

*Author to whom correspondence should be addressed.

**1,4-Diaza-1,3-butadienes, the simplest members of the α-diimines have the general formula RN=C(R′)–C(R″)=NR and an important subgroup of this class is RN=CH–CH=NR. For economy of space, if the R group is specifically stated, then the form R substituent-DAB is used and this implies proton substitution at the α-diimine carbon atoms, e.g. t-Bu–N=CH–CH=N–t-Bu becomes t-Bu–DAB. Abbreviations for the R groups in R–DAB or other molecules used throughout this paper are i-Pr = iso-propyl, t-Bu = tert. butyl, Ph = phenyl, Me = methyl.

0020-1693/88/$3.50

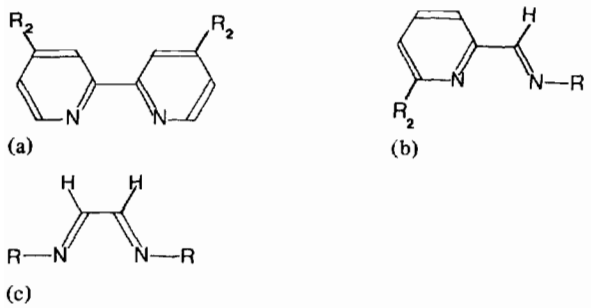

Fig. 1. α-diimines: 2,2'-bipyridine (a) (bipy, $R_2 = H$; bipy', $R_2 = CH_3$), pyridine-2-carbaldehydeimine (b) (R–PyCa, $R_2 = H$; R–PyCa', $R_2 = CH_3$) and 1,4-diaza-1,3-butadiene (c) (R–DAB).

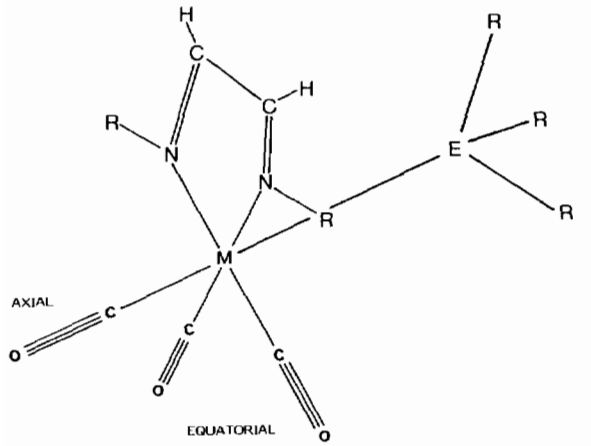

Fig. 2. General molecular geometry of the complexes $[Ph_3EM(CO)_3(\alpha\text{-diimine})]$.

Sn, Pb). In this article we present the spectroscopic data of the complexes $[(C_6H_5)_3EM(CO)_3(\alpha\text{-diimine})]$ (M = Mn, E = Ge, Sn, Pb; M = Re, E = Sn; α-diimine = bipy, R–PyCa or R–DAB) which are indispensable for an understanding or their photochemical behaviour [11].

Previous work on some of these complexes has been done by Wrighton and co-workers [12] who described the ground- and excited-state oxidation–reduction chemistry.

The structures of the α-diimine ligands used and of their complexes are shown in Figs. 1 and 2, respectively.

Experimental

Materials and Apparatus

^1H and ^{119}Sn NMR spectra were obtained on a Bruker WM 250 spectrometer, and ^{31}P NMR spectra on a Varian XL-100-15 spectrometer. IR spectra were recorded with a Nicolet 7199B FT-IR interferometer with a liquid nitrogen cooled Hg-Cd-Te-detector. Electronic absorption spectra were measured on a Perkin-Elmer Lambda 5 spectrophotometer and the rR spectra on a Jobin-Yvon HG2S Ramanor. The exciting sources were a SP model 171 Argon-ion laser and a model CR 490 tunable dye-laser with Rhodamine 110 or Coumarin 6 in ethylene–glycol as dyes. An Anaspec 300-S with a bandpass of 0.4 nm was used as premonochromator. The rR spectra were recorded from dispersions of the compounds in potassium nitrate disks at 110 K [13].

Elemental analyses were obtained by the section Elemental Analysis of the Institute for Applied Chemistry, TNO, Utrecht, The Netherlands. All preparations were done in an atmosphere of purified nitrogen, using carefully dried solvents. $Mn_2(CO)_{10}$ and $Re_2(CO)_{10}$ were purchased from Strem Chemicals and used without purification. R–DAB and R–PyCa ligands were prepared according to literature methods [14]. Phen and bipy were purchased from Merck.

Synthesis of $[Ph_3EM(CO)_3(\alpha\text{-diimine})]$ (E = Ge, Sn, Pb, M = Mn; E = Sn, M = Re)

These complexes were prepared according to published or derived methods [12]. First of all the $[BrM(CO)_3(\alpha\text{-diimine})]$ (M = Mn, Re) [15] complexes were reduced with excess $Na/K_{2.8}$ alloy in sufficient freshly distilled THF. After complete reduction, which was monitored by IR, the excess of Na/K alloy was filtered off, followed by addition of the appropriate Ph_3EX (E = Ge, Sn, Pb; X = Cl, Br).

$[Ph_3SnMn(CO)_3(i\text{-}Pr\text{–}DAB)]$

Anal. Found: C, 55.22; H, 5.11; N, 4.05; O, 6.66. Calc. for $C_{29}H_{31}MnN_2O_3Sn$: C, 55.36; H, 4.97; N, 4.45; O, 7.63%. IR ν(CO) (THF; 293 K): 1993(s), 1916(m), 1901(m) cm^{-1}. ^1H NMR ($CDCl_3$; 293 K) δ (multiplicity, integral): 0.96 (d, 6H)/1.48 (d, 6H), 4.48 (m, 2H), 7.29 (m, 9H), 7.43 (d, 6H), 7.78 (s, 2H) ppm.

$[Ph_3SnMn(CO)_3(t\text{-}Bu\text{–}DAB)]$

Anal. Found: C, 55.90; H, 5.47; N, 4.08; O, 6.76. Calc. for $C_{31}H_{35}MnN_2O_3Sn$: C, 56.65; H, 5.37; N, 4.26; O, 7.30%. IR ν(CO) (THF; 293 K): 1990(s), 1912(m), 1892(m) cm^{-1}. ^1H NMR ($CDCl_3$; 293 K) δ: 1.49 (s, 18H), 7.23 (m, 9H), 7.44 (d, 6H), 7.57 (s, 2H) ppm.

$[Ph_3SnMn(CO)_3(i\text{-}Pr\text{–}PyCa')]$

Anal. Found: C, 55.87; H, 4.48; N, 4.12; O, 7.61. Calc. for $C_{31}H_{29}MnN_2O_3Sn$: C, 57.18; H, 4.49; N, 4.30; O, 7.37%. IR ν(CO) (THF; 293 K): 1986(s), 1905(m), 1890(m) cm^{-1}. ^1H NMR ($CDCl_3$: 293 K) δ: 1.04 (d, 3H)/1.65 (d, 3H), 2.75 (s, 3H), 4.64 (m, 1H), 7.26 (m, broad, 18H), 8.09 (s, 1H) ppm.

[$Ph_3SnMn(CO)_3$(bipy')]

Anal. Found: C, 59.38; H, 4.88; N, 4.13; O, 7.04. Calc. for $C_{33}H_{27}MnN_2O_3Sn$: C, 58.88; H, 4.04; N, 4.16; O, 7.13%. IR ν(CO) (THF; 293 K): 1985(s), 1901(m), 1888(m) cm^{-1}. ^1H NMR ($CDCl_3$; 293 K) δ: 2.52 (s, 6H), 6.94 (d, 2H), 7.18 (m, 9H), 7.44 (d, 6H), 7.68 (s, 2H), 8.93 (d, 2H) ppm.

[$Ph_3SnMn(CO)_3$(en')]

IR ν(CO) (THF; 293 K): 1981(s), 1898(m), 1857-(m) cm^{-1}.

[$Ph_3GeMn(CO)_3$(i-Pr–DAB)]

IR ν(CO) (THF; 293 K): 1992(s), 1910(m), 1893-(m) cm^{-1}.

[$Ph_3PbMn(CO)_3$(i-Pr–DAB)

IR ν(CO) (THF; 293 K): 1995(s), 1918(m), 1908(m) cm^{-1}.

[$Ph_3SnRe(CO)_3$(t-Bu–DAB)]

Anal. Found: C, 47.31; H, 4.61; N, 3.52; O, 6.20. Calc. for $C_{31}H_{35}N_2O_3ReSn$: C, 47.22; H, 4.47; N, 3.55; O, 6.09%. IR ν(CO) (THF; 293 K): 2003(s), 1909(m), 1901(m) cm^{-1}. ^1H NMR ($CDCl_3$; 293 K) δ: 1.46 (s, 18H), 7.18 (m, 9H), 7.39 (d, 6H), 7.97 (s, 2H) ppm.

[$Ph_3SnRe(CO)_3$(i-Pr–PyCa)]

Anal. Found: C, 46.47; H, 3.62; N, 3.55; O, 6.21. Calc. for $C_{30}H_{27}N_2O_3ReSn$: C, 46.89; H, 3.54; N, 3.65; O, 6.25%. IR ν(CO) (THF; 293 K): 1997(s), 1901(m, broad) cm^{-1}. ^1H NMR ($CDCl_3$; 293 K) δ: 1.21 (d, 3H)/1.46 (d, 3H), 4.36 (m, 1H), 7.00 (t, 1H), 7.13 (m, 9H), 7.20 (d, 6H), 7.44 (d, 1H), 7.62 (t, 1H), 8.38 (s, 1H), 8.98 (d, 1H) ppm.

[$Ph_3SnRe(CO)_3$(bipy')]

IR ν(CO) (THF; 293 K): 1995(s), 1895 (m, broad) cm^{-1}. ^1H NMR ($CDCl_3$; 293 K) δ: 2.44 (s, 6H), 6.92 (d, 2H), 7.04 (m, 9H), 7.10 (d, 6H), 7.59 (s, 2H), 8.84 (d, 2H) ppm.

i-Pr-DAB

^1H NMR ($CDCl_3$: 293 K) δ: 1.24 (d, 12H), 3.43 (m, 2H), 7.93 (s, 2H) ppm.

t-Bu-DAB

^1H NMR ($CDCl_3$; 293 K) δ: 1.30 (s, 18H), 7.93 (s, 2H) ppm.

i-Pr-PyCa

^1H NMR ($CDCl_3$; 293 K) δ: 1.27 (d, 6H), 3.43 (m, 1H), 7.04 (t, 1H), 7.27 (t, 1H), 8.01 (d, 1H), 8.38 (s, 1H), 8.60 (d, 1H) ppm. This latter resonance is absent in i-Pr-PyCa': δ(CH_3-group): 1.96 (s, 3H) ppm.

bipy'

^1H NMR ($CDCl_3$; 293 K) δ: 2.51 (s, 6H), 7.19 (d, 2H), 8.30 (s, 2H), 8.60 (d, 2H) ppm.

Photochemical Preparation of [$Ph_3SnMn(CO)_2$(t-Bu–DAB)(PPh_3)]

[$Ph_3SnMn(CO)_3$(t-Bu–DAB)] (0.5 mmol) was dissolved in freshly distilled and deoxygenated THF (60 ml). An excess of PPh_3 (1 mmol) was added and the solution was irradiated with the blue/green line of an Ar ion laser (λ = 488 nm, $p \simeq 50$ mW) in a nitrogen atmosphere. After the reaction mixture had turned completely blue, the irradiation was stopped and checked by IR spectroscopy. Thereafter the solution was evaporated to dryness and washed twice by 100 ml benzene/hexane (1:4) to get rid of the excess PPh_3. Yield 98%. *Anal.* Found: C, 62.93; H, 5.65; N, 2.92; O, 4.17. Calc. for $C_{48}H_{50}MnN_2O_3PSn$: C, 64.67; H, 5.65; N, 3.14; O, 3.59%. IR ν(CO) (THF; 293 K): 1908(m), 1840(m) cm^{-1}. ^1H NMR ($CDCl_3$; 293 K in the dark) δ: 1.12 (s, 18H), 7.3–7.8 (m, broad, 30H), 8.26 (s, 2H) ppm. ^{31}P NMR (THF; 293 K) δ (with respect to 85% H_3PO_4): +23.6 ppm.

Crystal Structure Determination of [$Ph_3SnMn(CO)_3$-(t-Bu-DAB)]

Crystal data $C_{31}H_{35}MnN_2O_3Sn$, $M = 657.24$, monoclinic, space group $P2_1/c$, $a = 20.025(1)$, $b = 18.917(1)$, $c = 17.117(1)$ Å, $\beta = 112.120(0)°$, $V = 6006$ Å^3, $D_c = 1.44$ g/cm^3, $Z = 8$, $F(000) = 2672$, λ(Mo Kα) = 0.71069 Å, μ(Mo Kα) = 8.75 cm^{-1}.

4598 Reflections with $I > 2.5^*\sigma(I)$ were measured on a Nonius CAD 4 diffractometer (θ–2θ range) using graphite-monochromated Mo Kα radiation. No absorption corrections were applied. The positions of the heavy atoms Sn and Mn were derived from an E^2-Patterson synthesis. The remaining non-hydrogen atoms were obtained from subsequent ΔF syntheses. Refinement proceeded by means of block-diagonal least-squares calculations. The R value is 0.13 at this stage, due to pseudo symmetry in the Ph_3Sn parts of the molecules, preventing further refinement. This problem is still under study. The calculations were performed with the X-ray system [16] and PLUTO [17].

Results and Discussion

Molecular Orbital Scheme

In order to get more insight into the electronic structures of the complexes [$Ph_3EM(CO)_3$(α-diimine)] a comparison was made with the parent compounds [$Ph_3EM(CO)_5$] (E = Ge, Sn, Pb; M = Mn, Re) for which a qualitative molecular orbital (MO) diagram is depicted in Fig. 3A.

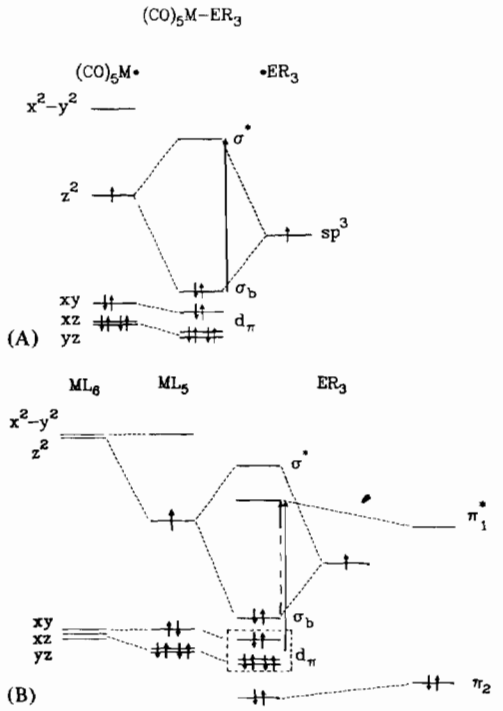

Fig. 3. (A): qualitative molecular orbital diagram of $[R_3EM(CO)_5]$; (B): qualitative molecular orbital diagram of $[R_3EM(CO)_3(\alpha\text{-diimine})]$.

The lowest-energy electronic transition of these complexes is the $\sigma_b \rightarrow \sigma^*$ (E–M) transition; the position of which depends on the sp^3 level of R_3E fragment [18].

It is known from other studies that especially the Sn–Mn bond in $[Ph_3SnMn(CO)_5]$ is remarkably strong with respect to halogenation reactions [19] under thermal conditions. Photochemical splitting of the metal–metal bond can be achieved by the use of UV radiation and in the presence of $P(OPh)_3$ many photoproducts have been formed [18].

When two carbonyl groups of the $M(CO)_5$ fragment are substituted by a bidentate ligand with a low-lying π^* orbital, such as an α-diimine ligand (Fig. 1), the MO diagram changes (Fig. 3B).

The lowest-energy transitions are now directed to this π^* orbital and may originate from the metal–metal bonding (σ_b) orbital as well as from the metal (d_π) orbitals not involved in the metal–metal bond. These transitions are responsible for the deep colours of these complexes. In the $[Ph_3EM(CO)_5]$ complexes (E = Ge, Sn, Pb; M = Mn, Re) the σ_b orbital is the HOMO. Substitution of the two carbonyl groups of the $M(CO)_5$ fragment by the α-diimine ligand, however, causes an increase of electron density at the central metal atom (M) [20]. As a result the metal d_π orbitals will be destabilized and (nearly) coincide with the σ_b orbital. This effect has been observed before in the Ultraviolet Photoelectron spectra of a series of d^7 metal–metal bonded carbonyls and their α-diimine derivatives [21].

X-ray Structure

Of special interest in the PLUTO picture (Fig. 4) of $[Ph_3SnMn(CO)_3(t\text{-Bu–DAB})]$ is the position of the t-Bu–DAB ligand. It was already shown by Staal *et al.* [22] and Kokkes *et al.* [6, 7] that this ligand coordinates σ-N, σ-N′ to, for example, Mn or Fe via its nitrogen lone-pairs. The crystal structure shows that the geometry is almost octahedral around the Mn atom and that the angle between the plane formed by Mn–N1–C19–C20–N2 and the Sn–Mn bond is 82°.

The configuration around the Sn atom is more or less tetrahedral, although the Ph groups are bent a few degrees away from the Mn atom. At this stage the R value is still 0.13 due to pseudosymmetry between the Ph_3Sn parts of different molecules. Because of this, some uncertainty still exists in the atom positions, which is, however, restricted to the atoms of the phenyl rings. Although this problem is still the subject of a detailed crystallographic study, further refinement will certainly not influence the bond lengths collected in Table I and also not change the PLUTO structure presented in Fig. 4. This structure agrees with those published for $[R_3EM(CO)_5]$ complexes [23].

TABLE I. Some Selected Bond Lengths (Å) of $[Ph_3SnMn(CO)_3(t\text{-Bu–DAB})]$

Sn1–Mn1	2.70(1)
Mn1–N1/N2	2.10(2) (mean)
Mn1–C21/C22/C23	1.85(1) (mean)
N1/N2–C19/C20	1.29(2) (mean)

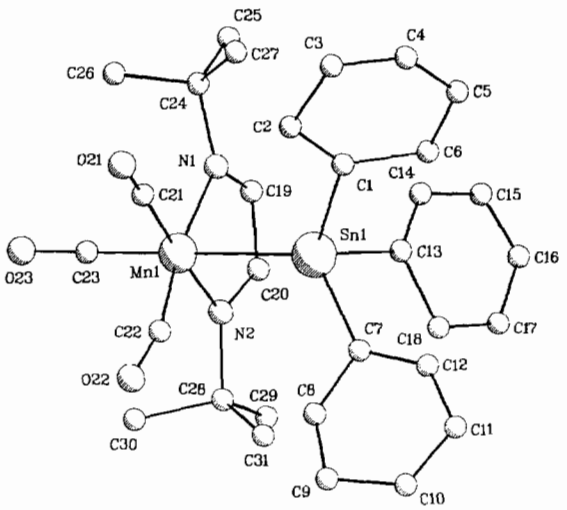

Fig. 4. PLUTO drawing of $[Ph_3SnMn(CO)_3(t\text{-Bu–DAB})]$.

Infrared and (^1H, ^{119}Sn and ^{31}P) NMR Spectra

The three IR bands in the 1800–2000 cm^{-1} region (see 'Experimental'), can be assigned to the three IR active CO stretching modes $2a' + a''$ (C_s symmetry). Although the vibrations of the axial and equatorial carbonyl groups in $[Ph_3EM(CO)_3(\alpha\text{-diimine})]$ will be mixed to some extent we can still distinguish the band around 2000 cm^{-1} from those at lower frequencies by the reasoning used for the corresponding $[ReX(CO)_3(\alpha\text{-diimine})]$ (X = Cl, Br, I) [3b] and $[M(CO)_3(\alpha\text{-diimine})(L)]$ (M = Cr, Mo, W; L = PR_3, CNR) [5, 24] complexes. The highest frequency band is hardly influenced by variation of the α-diimine ligand from R–DAB via R–PyCa to bipy contrary to the two IR absorptions at lower frequencies. Besides, the former band belongs to the only CO stretching mode which is observed in the rR spectra (*vide infra*) and which is therefore assigned to $\nu(CO)_{ax}$ (a'). The remaining two bands of equal intensity between 1890 and 1920 cm^{-1} belong to $\nu(CO)_{eq}^{asym}$ (a'') and $\nu(CO)_{eq}^{sym}$ (a'), respectively, the latter having the lowest frequency. The less electron-withdrawing character of the Ph_3E group with respect to the halide in $[XM(CO)_3(\alpha\text{-diimine})]$ is reflected in the lower frequencies of the CO stretching modes. The influence of π-backbonding to the α-diimine ligand can be seen from the higher CO stretching frequencies of $[Ph_3EM(CO)_3(\alpha\text{-diimine})]$ with respect to those of $[Ph_3SnMn(CO)_3(en')]$ (en' = tetramethylethylenediamine). This π-backbonding, which is also reflected in a decrease of ν(CN) of the α-diimine ligand upon coordination, increases in the order bipy < R–PyCa < R–DAB. Variation of the post-transition metal from Ge to Sn and Pb hardly influences the frequencies of the CO stretching modes which means that these complexes have a similar charge distribution.

Photosubstitution of the axial CO ligand in $[Ph_3SnMn(CO)_3(t\text{-Bu–DAB})]$ by PPh_3 causes the disappearance of $\nu(CO)_{ax}$ and a shift of the equatorial CO stretching modes and of ν(CN) of the t-Bu–DAB ligand to lower frequencies. In a following article [11] the properties of these photosubstitution products will be discussed in more detail.

^1H NMR Spectra

On complexation the imine proton resonances of the α-diimine ligands shift upfield ('experimental'), indicating a strong π-backbonding from the metal to these ligands. Furthermore, the proton resonances of the phenyl groups of Sn hardly change throughout the series which means that hardly any charge shift takes place towards or from the phenyl groups.

^{119}Sn NMR Spectra

In order to get more information about the charge distribution in these complexes, their ^{119}Sn NMR spectra were studied. During the last few years the application of multinuclear NMR spectroscopy has become rather popular and several review articles have already appeared [25].

TABLE II. ^{119}Sn NMR Chemical Shifts[a] of the $[Ph_3SnM(CO)_3(\alpha\text{-diimine})]$ Complexes

$[Ph_3SnMn(CO)_3(t\text{-Bu–DAB})]$	+12.2
$[Ph_3SnMn(CO)_3(i\text{-Pr–DAB})]$	−7.3
$[Ph_3SnMn(CO)_3(i\text{-Pr–PyCa}')]$	+6.0
$[Ph_3SnMn(CO)_3(bipy')]$	+15.0
$[Ph_3SnRe(CO)_3(t\text{-Bu–DAB})]$	−18.4

[a]In C_6H_6 solutions at 293 K; shifts are in ppm relative to Me_4Sn.

As can be seen from Table II the ^{119}Sn resonances are extremely sensitive to small changes in the charge distribution of the complex. This can be seen, for example, from the values for $[Ph_3SnMn(CO)_3(R\text{–DAB})]$ (R = i-Pr or t-Bu). The minor change, caused by the substitution of the i-Pr group by t-Bu, far away from the Sn atom, already causes an increase of δ by 19.5 ppm. Apparently, the increase of electron density on Mn, caused by the extra CH_3 group of t-Bu–DAB with respect to i-Pr, results in a compensating positive δ shift for the ^{119}Sn nucleus. In the series $[Ph_3SnMn(CO)_3(\alpha\text{-diimine})]$ the same trend is observed since the decrease of π-backbonding capability on going from R–DAB to i-Pr–PyCa' and bipy', again results in an increase of electron density on Mn and a constant increase of the chemical shift of ^{119}Sn.

^{31}P NMR Spectra

The PPh_3 ligands in the photosubstitution products $[Ph_3SnMn(CO)_2(\alpha\text{-diimine})(PPh_3)]$ ('Experimental') hardly show any dependence on the α-diimine ligand in their change of ^{31}P chemical shift (Δ) on coordination. However, the absolute value of Δ (29.7) ppm is much smaller than reported for e.g. $[Mo(CO)_3(\alpha\text{-diimine})(PPh_3)]$ [3a] which result points to a relatively weak Mn–P bond. The weakness of this bond is indeed demonstrated by the fast backreaction of these photoproducts with CO to their parent compounds.

Electronic Absorption Spectra

Some typical spectra are shown in Figs. 5 and 6 and the data are collected in Table III. Only the bands above 320 nm are shown together with their solvatochromism.

The strongly solvent dependent absorption bands can be assigned with the aid of the simplified MO diagram depicted in Fig. 3B and postulated by Wrighton *et al.* [12].

These authors assigned the lowest-energy absorption band to an electronic transition from the metal–metal bonding orbital (σ_b) to the lowest π^* level

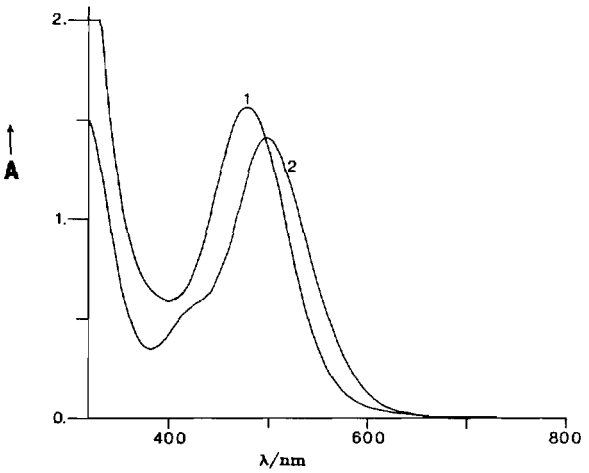

Fig. 5. Lowest-energy absorption bands of $[Ph_3SnMn(CO)_3$-(t-Bu–DAB)] (1 = acetonitrile; 2 = cyclohexane).

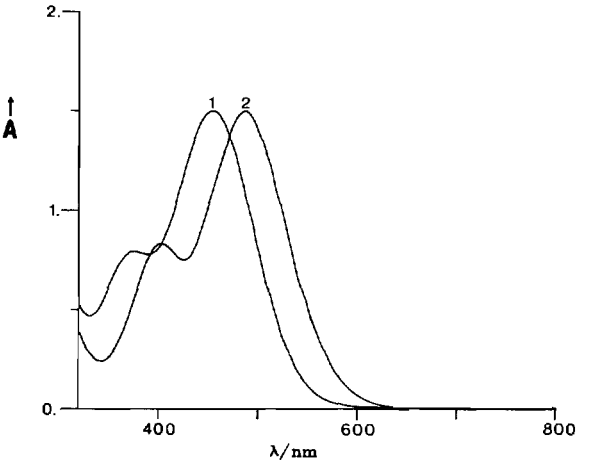

Fig. 6. Lowest-energy absorption bands of $[Ph_3SnRe(CO)_3$-(t-Bu–DAB)] (1 = acetonitrile; 2 = cyclohexane).

(π^*_1) of the α-diimine ligand ($\sigma_b \rightarrow \pi^*_1$). This assignment is however rather unlikely for the following reasons. First of all, the σ_b orbital will hardly overlap with the π^*_1 level and a transition between these orbitals can therefore not account for the high intensity of this absorption band. Secondly, the rR spectra, which will be discussed below, closely resemble those of the mononuclear analogues [ReX-$(CO)_3$(α-diimine)] (X = Cl, Br, I) [3b] and [$M(CO)_4$-(α-diimine)] (M = Cr, Mo, W) [3a, 4a, 4b]. For one of the [$Ph_3SnRe(CO)_3$(α-diimine)] complexes only a weak rR effect is observed for the metal–metal vibration. We therefore assign this low-energy band to the MLCT transitions from the metal-d_π orbitals not involved in the metal–metal bond to $\pi^*_1(d_\pi \rightarrow \pi^*_1)$. This assignment agrees with the one given by Kokkes *et al.* [6] and Staal *et al.* [22] for the low-energy band of the corresponding complexes [$(CO)_5$-$MM'(CO)_3$(α-diimine)] (M, M' = Mn, Re). The presence of more than one MLCT transition within this band (see Fig. 3B) is evident from the appearance of a shoulder at the high-energy side in apolar solvents and at lower temperatures. One has to realize that the HOMO of these complexes may still be the σ_b orbital as has been observed in the Ultraviolet Photoelectron Spectra of analogous complexes [21, 26]. From the solvatochromic behaviour of these MLCT transitions (Δ, Table III) it can be concluded that the shift Δ increases in the order R–DAB < R–Py-Ca < bipy in agreement with a decrease of π-back-bonding capacities in this order.

Substitution of CO_{ax} by PR_3 in [$Ph_3SnMn(CO)_3$-(t-Bu–DAB)] causes an increase of electron density on Mn and as a result not only a shift to lower energy of the MLCT band, but also complete loss of solvatochromic (Δ = 0) behaviour.

Resonance Raman Spectra

In order to get more information about the character of the MLCT transitions and the properties of

TABLE III. UV–Vis Spectral Data of [$Ph_3EM(CO)_3$(α-diimine)] Complexes (λ [nm]; ε [M^{-1} l cm^{-1}] in parentheses)

	MLCT transitions			Δ[a]
	$\lambda^{max}_{c\text{-hexane}}$		$\lambda^{max}_{acetonitrile}$	
[$Ph_3GeMn(CO)_3$(i-Pr–DAB)]	500	373[b]	481 (4550)	19
[$Ph_3SnMn(CO)_3$(t-Bu–DAB)]	499	421[b]	479 (5100)	20
[$Ph_3PbMn(CO)_3$(i-Pr–DAB)]	507	438[b]	486 (4200)	21
[$Ph_3SnMn(CO)_3$(i-Pr–PyCa')]	534	332	488 (4650)	46
[$Ph_3SnMn(CO)_3$(bipy')	537	334	477 (2200) 338 (4800)	60
[$Ph_3SnMn(CO)_2$(t-Bu–DAB)(PPh_3)]	596	399[c]	591 (3400) 400 (5600)	5
[$Ph_3SnRe(CO)_3$(t-Bu–DAB)]	487	403	454 (5200) 376 (2700)	33
[$Ph_3SnRe(CO)_3$(i-Pr–PyCa)]	510	376	456 (5900) 338 (2700)	54
[$Ph_3SnRe(CO)_3$(bipy')]	500[c]		434 (4150)	66

[a] $\Delta = \lambda^{max}_{c\text{-hexane}} - \lambda^{max}_{acetonitrile}$ in nm of the lowest MLCT band. [b]Shouder. [c]Sparingly soluble.

of the excited states, the rR spectra of the $[Ph_3Sn-M(CO)_3(\alpha\text{-diimine})]$ complexes and of the photoproduct $[Ph_3SnMn(CO)_2(t\text{-Bu–DAB})(PPh_3)]$ were investigated. During these measurements the frequency of the exciting laser line (nearly) coincided with the maximum of the low-energy absorption band. Because of the strong photosensitivity of these complexes in solution [11, 12], the spectra were measured from KNO_3 disks at 110 K [13], two of them being illustrated in Figs. 7 and 8.

Resonance enhancement is observed for several stretching modes of the α-diimine ligand and for one of the CO stretching mode in the case of the Mn complexes. In the low-frequency region (70–700 cm^{-1}) weak rR effects are observed for several metal–ligand stretching modes and for M–CO deformation modes. Between 700 and 1300 cm^{-1} mainly α-diimine deformation modes are Raman active but these vibrations only show very weak rR effects.

The strong rR effects observed for $\nu_s(CN)$, the symmetrical CN stretching mode of the R–DAB and R–PyCa ligands and for the pyridine ring stretching modes of the R–PyCa and bipy ligands, confirm the assignment of the lowest-energy absorption band to electronic transitions from the metal to the lowest π^* level (π^*_1) of the α-diimine ligand.

Two important conclusions can be drawn from these rR spectra. First of all, for only one of the complexes a weak rR effect is observed for the metal–metal vibration (ν(Sn–Re) of $[Ph_3SnRe(CO)_3(t\text{-Bu–DAB})]$ at 133 cm^{-1}). This means that the metal–metal bond is not or hardly affected during these MLCT transitions. These transitions will therefore not take place from the metal–metal bonding orbital σ_b but from the metal d_π orbitals not involved in the metal–metal bond. This conclusion is supported by the close similarity between these spectra and those of the mononuclear analogues $[ReX(CO)_3(\alpha\text{-diimine})]$ (X = Cl, Br) [3b] and $[M(CO)_4(\alpha\text{-diimine})]$ (M = Cr, Mo, W) [3a, 4a–c].

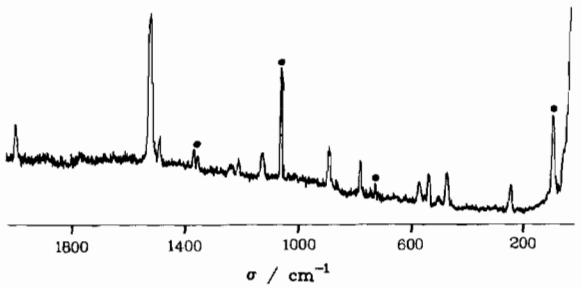

Fig. 7. Resonance Raman spectrum of $[Ph_3SnMn(CO)_3(t\text{-Bu–DAB}]$ (KNO_3 disk at 110 K; λ_{exc} = 514.5 nm; p = 100 mW).

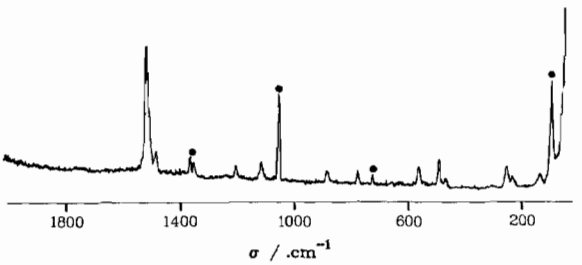

Fig. 8 Resonance Raman spectrum of $[Ph_3SnRe(CO)_3(t\text{-Bu–DAB})]$ (KNO_3 disk at 110 K; λ_{exc} = 514.5 nm; p = 120 mW).

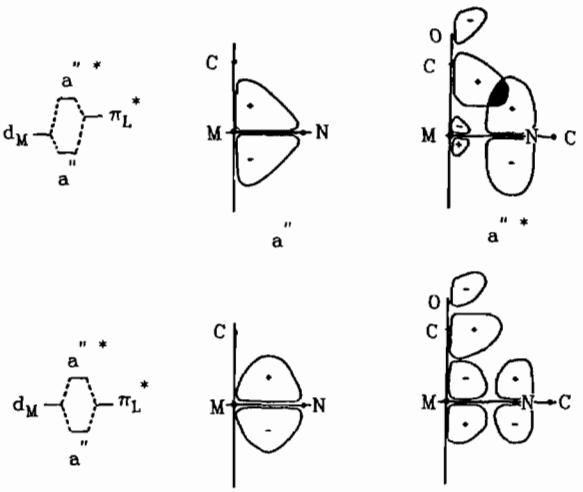

Fig. 9. Excited state 'through-space' interaction of metal d_π, α-diimine π^*_1 and axial carbonyl π^* orbitals in the case of the weak (top) and strong (bottom) metal (d_π)–α diimine (π^*_1) mixing.

A second important feature is the observation of a rR effect for just one CO stretching mode at about 2000 cm^{-1} in the case of the manganese complexes. This vibration which belongs to the carbonyl ligand *trans* to the tin atom ($\nu(CO)_{ax}$) is not observed in the spectra of the corresponding Re complexes. A similar phenomenon has been observed for the corresponding $[M(CO)_4(\alpha\text{-dimine})]$ (M = Cr, Mo, W) complexes which usually only show a strong rR effect for one of the ν(CO)s in the case of M = Cr [3b, 4a–c]. The frequencies of $\nu(CO)_{ax}$ and $\nu_s(CN)$ are 30–40 cm^{-1} lower than those for the corresponding modes of $[MX(CO)_3(\alpha\text{-diimine})]$ (M = M, Re; X = Cl, Br) [3b]. These shifts are most pronounced for the t-Bu–DAB complexes.

The observation of a resonance enhanced $\nu(CO)_{ax}$ in the case of the manganese complexes $[Ph_3SnMn(CO)_3(\alpha\text{-diimine})]$ can be explained with the model developed before [3a] and schematically illustrated in Fig. 9. When the MLCT transition ($d_\pi \rightarrow \pi^*_1$) has a strong MLCT character as, for example, in the case of the bipy complexes, the mixing between the d_π and π^*_1 orbitals will be weak and the excited state will have its largest electron density at the N atoms of the α-diimine ligand. Through-space

overlap can then take place between π^*_1 and a π^* orbital of the axial carbonyl ligand.

Excitation of an electron into π^*_1 causes an increase of electron density at the axial carbonyl which in turn involves a rR effect for its stretching vibration. No such overlap can occur with the π^* orbitals of the two equatorial CO groups. When there is a strong mixing between the metal d_π and α-diimine π^*_1 orbitals (π-backbonding) as in the case of the R–DAB complexes (Fig. 9 bottom), the interaction between the MLCT state and a π^* orbital of CO_{ax} will be repulsive. Thus, no delocalization of negative charge over the CO ligand will take place and no rR effect is observed for $\nu(CO)_{ax}$. This explains the decrease of rR intensity of $\nu(CO)_{ax}$ on going from the bipy to R–PyCa and R–DAB complexes [3]. Not only the strength of mixing between the d_π and π^*_1 orbitals is of importance here, the size of the metal also influences the delocalization of the excited state. When the size of the metal increases on going from Mn to Re, through-space overlap between π^*_1 and $\pi^*(CO_{ax})$ will decrease. This in turn will cause a decrease of rR intensity of $\nu(CO)_{ax}$.

Although rR spectra have been recorded with different exciting laser lines, no reliable excitation profiles could be obtained since the complexes were inhomogeneously dissipated in the KNO_3 disks. Moreover, photodecomposition became a severe problem at wavelengths longer than 520 nm. The only important feature of the rR spectrum of the photoproduct $[Ph_3SnMn(CO)_2(t\text{-}Bu\text{–}DAB)(PPh_3)]$ is the absence of $\nu(CO)_{ax}$.

Acknowledgements

We wish to thank Mr D. Heijdenrijk, Mr K. Goubitz and Prof. Dr. B. O. Loopstra of the Laboratorium voor Kristallografie for measuring and solving the crystal structure.

References

1 G. van Koten and K. Vrieze, *Adv. Organomet. Chem.*, *21*, 153 (1982).
2 (a) L. H. Staal, D. J. Stufkens and A. Oskam, *Inorg. Chim. Acta*, *26*, 255 (1978); (b) L. H. Staal, D. J. Stufkens and A. Terpstra, *Inorg. Chim. Acta*, *34*, 97 (1979).
3 (a) R. W. Balk, D. J. Stufkens and A. Oskam, *Inorg. Chim. Acta*, *28*, 133 (1978); *34*, 267 (1979); (b) R. W. Balk, D. J. Stufkens and A. Oskam, *J. Chem. Soc., Dalton Trans.*, 1124 (1981).
4 (a) H. K. van Dijk, P. C. Servaas, D. J. Stufkens and A. Oskam, *Inorg. Chim. Acta*, *104*, 179 (1985); (b) P. C. Servaas, H. K. van Dijk, Th. L. Snoeck, D. J. Stufkens and A. Oskam, *Inorg. Chem.*, *24*, 4494 (1985); (c) D. J. Stufkens, *J. Mol. Struct.*, *79*, 67 (1982); (d) H. tom Dieck and I. W. Renk, *Chem. Ber.*, *104*, 92 (1971); (e) H. tom Dieck, K.-D. Franz and F. Hohmann, *Chem. Ber.*, *108*, 163 (1975).
5 R. W. Balk, D. J. Stufkens and A. Oskam, *Inorg. Chem.*, *19*, 3015 (1980).
6 M. W. Kokkes, Th. L. Snoeck, D. J. Stufkens, A. Oskam, M. Cristophersen and C. H. Stam, *J. Mol. Struct.*, *131*, 11 (1985).
7 M. W. Kokkes, D. J. Stufkens and A. Oskam, *J. Chem. Soc., Dalton Trans.*, 439 (1983); 1005 (1984).
8 R. W. Balk, D. J. Stufkens and A. Oskam, *J. Chem. Soc., Dalton Trans.*, 275 (1982).
9 (a) M. W. Kokkes, D. J. Stufkens and A. Oskam, *Inorg. Chem.*, *24*, 2934 (1985); (b) M. W. Kokkes, W. G. J. de Lange, D. J. Stufkens and A. Oskam, *Inorg. Chem.*, *24*, 4411 (1985); (c) D. L. Morse and M. S. Wrighton, *J. Am. Chem. Soc.*, *98*, 3931 (1976).
10 H. K. van Dijk, D. J. Stufkens, A. Oskam, M. Rotteveel and D. Heijdenrijk, *Organometallics*, *6*, 1665 (1987).
11 R. R. Andréa, W. G. J. de Lange, D. J. Stufkens and A. Oskam, to be published.
12 J. C. Luong, R. A. Faltyrek and M. S. Wrighton, *J. Am. Chem. Soc.*, *101*, 1597 (1979); *102*, 7892 (1980).
13 R. J. H. Clark and Ph. C. Turtle, *Inorg. Chem.*, *17*, 2527 (1978).
14 H. Bock and H. tom Dieck, *Chem. Ber.*, *100*, 228 (1967).
15 L. H. Staal, A. Oskam and K. Vrieze, *J. Organomet. Chem.*, *170*, 235 (1979).
16 J. M. Stewart, The X-ray system, *Technical Report TR 446*, Computer Service Center, University of Maryland, College Park, Md., 1976.
17 W. D. S. Motherwell, 'PLUTO', program for plotting crystal and molecular structures, University of Cambridge, 1976.
18 S. Onaka, Y. Kondo, N. Furuichi, K. Toriumi and T. Ito, *Bull. Chem. Soc. Jpn.*, *56*, 87 (1983).
19 J. R. Chipperfield, J. Ford and D. E. Webster, *J. Organomet. Chem.*, *102*, 417 (1975).
20 R. R. Andréa, J. N. Louwen, M. W. Kokkes, D. J. Stufkens and A. Oskam, *J. Organomet. Chem.*, *281*, 273 (1985).
21 R. R. Andréa, D. J. Stufkens and A. Oskam, *J. Organomet. Chem.*, *290*, 63 (1985).
22 L. H. Staal, G. van Koten and K. Vrieze, *J. Organomet. Chem.*, *175*, 73 (1979).
23 B. T. Kilbourn, T. L. Blundell and H. M. Powell, *J. Chem. Soc., Chem. Commun.*, 444 (1965).
24 R. W. Balk, D. J. Stufkens and A. Oskam, *Inorg. Chim. Acta*, *48*, 105 (1981).
25 (a) R. K. Harris, J. D. Kennedy and W. McFarlane, in R. K. Harris and B. E. Mann (eds.), 'NMR and the Periodic Table', Academic Press, London, 1978; (b) P. J. Smith and L. Smith, *Inorg. Chim. Acta Rev.*, *7*, 11 (1973); (c) R. Hani and R. A. Geanangel, *Coord. Chem. Rev.*, *44*, 229 (1982).
26 J. N. Louwen, R. R. Andréa, D. J. Stufkens and A. Oskam, *Z. Naturforsch., Teil B*, *38*, 194 (1983).